*Journal of the Meteorological Society of Japan*, Vol. 96, No. 4, pp. 415−423, 2018
DOI:10.2151/jmsj.2018-046


# NOTES AND CORRESPONDENCE

# A Systematic Tropospheric Dry Bias in the Tropics in CMIP5 Models: Relationship between Water Vapor and Rainfall Characteristics

**Hiroshi G. TAKAHASHI**

*Department of Geography, Tokyo Metropolitan University, Hachioji, Japan*
*Japan Agency for Marine-Earth Science and Technology (JAMSTEC), Yokohama, Japan*

*(Manuscript received 22 February 2018 in final form 9 May 2018)*

## Abstract

This study investigated the absolute values of column-integrated water vapor (precipitable water; PW) in the climate models used in the Coupled Model Intercomparison Project Phase 5 (CMIP5), in terms of the relationships between PW and precipitation characteristics. We identified that global mean PW values are systematically much lower in CMIP5 models than in observations. This dry bias is most profound over the tropical ocean. The dry bias is partly due to biases in sea surface temperatures in the CMIP5-coupled climate models. However, the dry bias is also present in Atmospheric Model Intercomparison Project (AMIP) experiments, which implies the existence of other factors. The relationship between PW and rainfall characteristics shows that rainfall occurs when water vapor levels are lower than in observations, particularly in models with a relatively strong dry bias. This suggests that the reproducibility of rainfall characteristics may be associated with the dry bias.

**Keywords** water vapor; rainfall characteristics; IPCC-AR5; tropics; climate variation

## 1. Introduction

Water vapor plays a major role in fluctuations in energy and water cycles. Furthermore, water vapor is the source of clouds and precipitation, which are essential components of the water cycle, and it induces variation in downward shortwave radiation at the surface. Water vapor is also a major greenhouse gas that affects the radiation budget, particularly that for downward longwave radiation at the surface.

Previous studies have examined long-term trends and interannual variation in water vapor. For example, Trenberth et al. (2005) investigated the trends and variability in column-integrated atmospheric water vapor (or precipitable water; PW) using a dataset from the NASA Water Vapor Project (NVAP; Randel et al. 1996), and found that PW increased over the tropical ocean in association with increases in sea surface temperatures (SSTs) from 1988 to 2001. The trend in PW over the tropical ocean (7.8 % $K^{-1}$) is governed by the Clausius-Clapeyron (CC) equation under the assumption of fairly constant relative humidity. In an earlier study, Wentz and Schabel (2000) reported a similar result (9.2 % $K^{-1}$) based on shorter observations of water vapor. These trends and variability were common in Coupled Model Intercomparison Project Phase 3 (CMIP3) climate models (e.g., Allan 2009).

Many studies have evaluated the reproducibility of clouds and precipitation in climate models (e.g., Jiang et al. 2012; Su et al. 2013). However, only a few studies have evaluated the reproducibility of water vapor in climate models. To improve the reproducibility of clouds and precipitation in global and regional climate models, it is important to understand the source of clouds and precipitation (i.e., water vapor).

Corresponding author: Hiroshi G. Takahashi, Department of Geography, Tokyo Metropolitan University, 1-1, Minami-oosawa, Hachioji, Tokyo 192-0397, Japan
E-mail: hiroshi3@tmu.ac.jp
J-stage Advance Published Date: 25 May 2018

Mears et al. (2007) examined the relationship between temperature and PW in climate models and found that the CC equation explained the long-term changes and interannual variation in the relationship fairly well. Su et al. (2013) discussed the reproducibility of clouds in climate models using related variables, such as SST and PW. In addition, John and Soden (2007) evaluated vertial profiles of the CMIP3 climate models, which indicates a large moist bias in the free atmosphere but a dry bias in the boundary layer. Tian et al. (2013) reported the similar characteristics also in CMIP5 climate models.

Trenberth et al. (2005) found an inconsistency in PW between the National Centers for Environmental Prediction/National Center for Atmospheric Research (NCEP/NCAR) and the 40-year Reanalysis (ERA40) of the European Centre for Medium-range Weather Forecasts (ECMWF). Takahashi et al. (2012) reported that PW was underestimated in seven reanalyses, excluding ERA40. This suggested the existence of water vapor biases in the climate models of the CMIP5 used for the Fifth Intergovernmental Panel on Climate Change assessment report (IPCC-AR5). To reiterate, PW in climate models has been poorly assessed.

Therefore, the primary purpose of this study was to investigate the bias in PW in the climate models of the CMIP5, based on a comparison with available global-scale PW observations. This study also investigated the causes of the bias in PW in the climate models, focusing on the relationship between water vapor and rainfall characteristics. Section 2 details the CMIP5 and observation datasets. Section 3 describes the common biases in column-integrated water vapor data. Possible explanations for these biases are provided in Section 4 and the conclusions are presented in Section 5.

## 2. Datasets

### *2.1 Model output*

We used the output from 21 different fully coupled ocean-atmosphere climate models (CGCM) in this study; the models are given in Fig. 1) The model results are available via the CMIP5 of the World Climate Research Programme (WCRP) (Taylor et al. 2012). The simulations considered here are of historical experiments that include historical changes in anthropogenic and natural forcing. This study used the monthly mean PW (*prw*), and precipitation (*pr*). The analysis period was from 1989 to 2005, because both observation datasets and model outputs are available for this period. Before calculating the multi-model mean (MMM), the spatial resolution of all values was unified in a 2.5° × 2.5° grid.

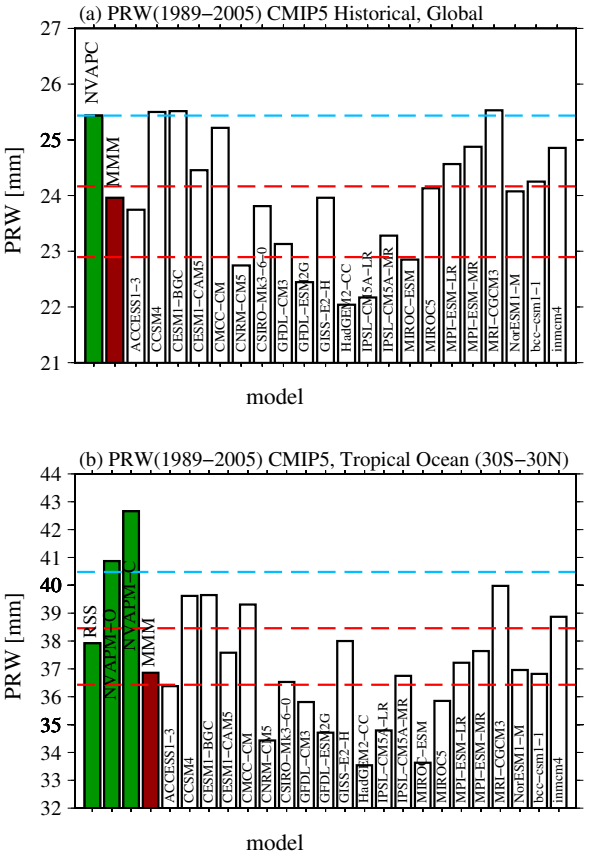


Fig. 1. (a) Global mean precipitable water (PW) amounts of the observations and simulations. Multi-model mean (MMM) indicates a 21 model-ensemble mean. The light-blue dashed line indicates the NVAP-M Climate (NVAP-C) observations. The upper (lower) red dashed lines indicate −5 % (−10 %) of the NVAP-C observations in (a). (b) Tropical oceanic mean PWs of the observations and simulations. The tropics were defined as the region from 30°S–30°N. Again, MMM indicates a 21 model-ensemble mean. The three observations (NVAP-C, NVAP-M Ocean [NVAP-O], and remote sensing systems [RSS]) are shown. The light-blue dashed line indicates the ensemble mean of the three observations over the tropical ocean. The upper (lower) red dashed line indicates −5 % (−10 %) of the three-ensemble mean over the tropical ocean in (b).

To examine the bias in SSTs in the CMIP5 climate models, we also used the output from 10 Atmospheric Model Intercomparison Project (AMIP) runs sim-

ulated by atmosphere-only global climate models (AGCMs), with the prescribed SST and sea ice data. Ten AMIP runs were obtained: CCSM4, CNRM-CM5, GFDL-CM3, IPSL-CM5A-LR, MIROC5, MPI-ESM-LR, MPI-ESM-MR, MRI-CGCM3, bcc-csm1-1, and inmcm4.

To calculate the average of PW over only the tropical ocean, the land area fraction (*sftlf*) for each model was used. This fraction was also converted in the 2.5° × 2.5° grid. When the land area fraction of a grid was less than 50 %, the grid was deemed an oceanic grid.

### *2.2 Observations*

The NVAP-MEaSUREs (NVAP-M; Vonder Haar et al. 2012) dataset was used for the PW observations. NVAP-M includes NVAP-M Climate (NVAP-C), NVAP-M Ocean (NVAP-O), and NVAP-M Weather (NVAP-S). NVAP-C is produced from input data and algorithms used consistently over time, and is the most suitable for climate research. NVAP-O is also suitable for climate research. However, NVAP-O covers only oceans. We did not use NVAP-S because its focus is not on climate, and therefore its long-term consistency is uncertain. NVAP-M covers the 22-year period from 1988 to 2009, although there are many missing PW values in 1988. Therefore, this study used the 17-year period from 1989 to 2005. NVAP-C PW is based on the Special Sensor Microwave Imager (SSMI), High-resolution Infrared Radiation Sounder (HIRS), and Atmospheric Infrared Sounder (AIRS) PW. An additional PW observation over the ocean, the remote sensing systems' (RSS) PW, was also used (Wentz 1997; Wentz et al. 2007) to qualify the uncertainty among the observations. The RSS PW was based on the SSMI and the Special Sensor Microwave Imager Sounder (SSMIS), which are satellite passive microwave radiometers. As discussed in Schröder et al. (2016), sources of data sets were different. In addition, the different merging processes were performed. To evaluate the simulated rainfall characteristics, we used monthly precipitation data from the Global Precipitation Climatology Project (GPCP) (ver. 2.2; Adler et al. 2003). This study used only the vertically integrated water vapor data because there are few vertically resolved observation datasets on water vapor at a global scale.

## 3. Results

### *3.1 Systematic dry bias of absolute value of PW*

To understand the bias in annual PW, we calculated the global mean PW, as simulated by the CMIP5 climate models and from observations. The climatological global mean PWs simulated by the CMIP5 climate models over the 17-year period from 1989 to 2005 were typically much lower than the observations (Fig. 1a). The 17-year climatological global mean PW of the NVAP-C observation was approximately 25.4 mm. This value is similar to the NVAP value (not shown), although the averaged period differs from that of NVAP-C. The MMM PW was approximately 23.9 mm, which was approximately 5.9 % drier than the observations. MMM PW and 12 of the 21 models had a dry bias exceeding 5 %. The deviation in the simulated PW ranged from approximately 22 to 25.5 mm. The observed value was almost outside this range, indicating that the dry bias is significant and common to the CMIP5 climate models.

Over the tropical ocean, the dry biases in the CMIP5 climate models were distinct (Figs. 1b, 2). RSS PW was much drier than NVAP-C, which indicates that the uncertainty among the PW observations is not small. Even considering the uncertainty of the observations between NVAP-C and RSS PWs (See also Section 3.2), the systematic dry bias in the CMIP5 climate models cannot be ignored, particularly over the tropical ocean (Fig. 1b).

### *3.2 Spatial pattern of model biases in PW*

This subsection examines the spatial distribution of the simulated and observed PW (Figs. 2a, b). Peaks in PW were observed around the Maritime Continent, equatorial North Pacific, and equatorial North Atlantic (Fig. 2a). The spatial maxima of the MMM simulated PW by the CMIP5 climate models agreed with the observations (Fig. 2b). The spatial distribution of PW simulated by each CMIP5 model was also similar to the observations (not shown).

To understand the spatial distribution of the bias in the simulated PW, we produced a spatial map of the differences in PW between the simulated and observed PWs (Fig. 2c). Dry biases in MMM were found over the entire tropics, and particularly over the higher SST regions (i.e., the warm pool region). Wet biases were observed over both the northeastern and southeastern Pacific in the tropics, where the SST was relatively low. This anomalous pattern of PW biases has been reported by Su et al. (2013). This study found that the absolute values of PW have strong dry biases. To further assess the spatial pattern of model biases in PW, that relative to RSS PW is also shown in Fig. 2d. The similar spatial pattern of model bias in PW can be found on the difference between MMM and RSS PWs, although the magnitude is smaller. The results in the previous studies and this study imply that the

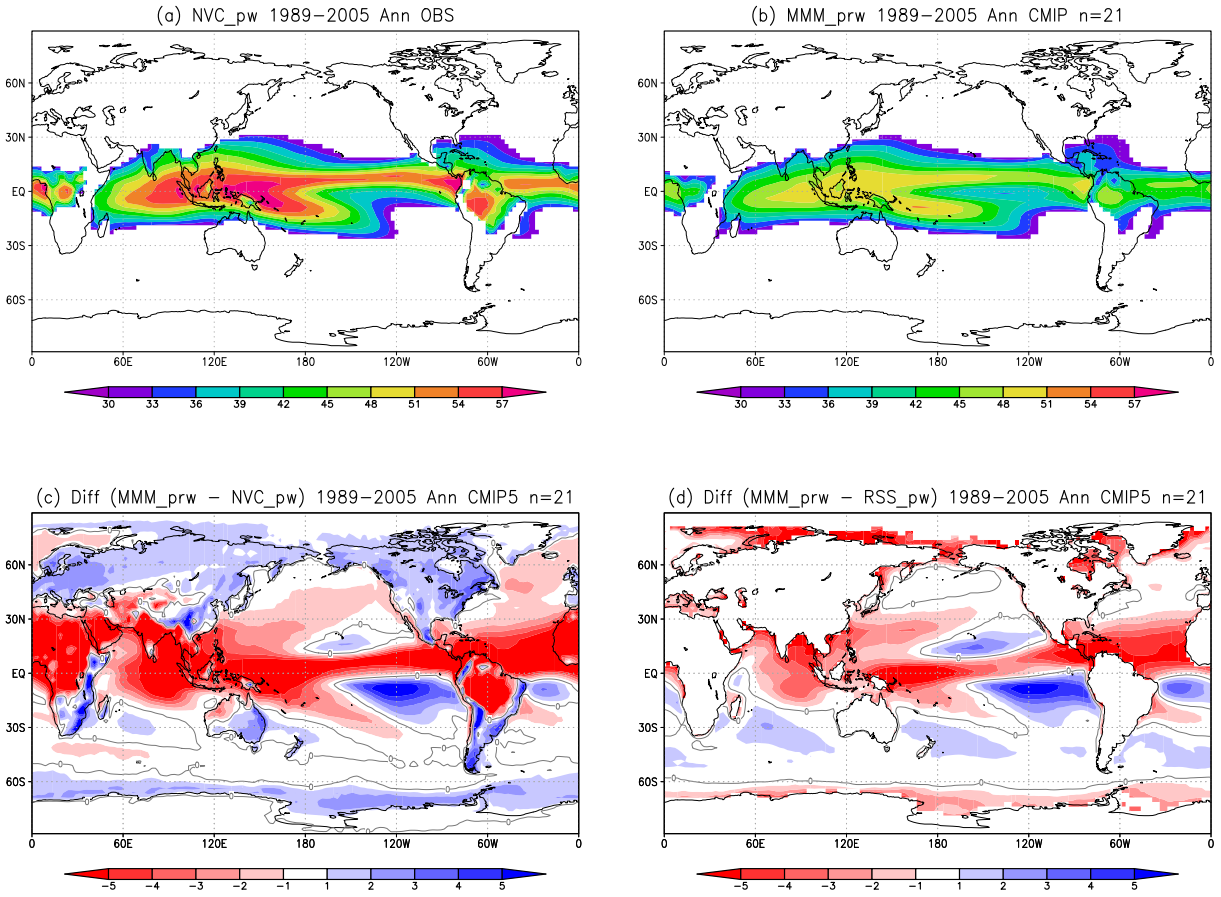


Fig. 2. (a) Climatology of the observed PW (NVAP-C) over the 17-year period from 1989 to 2005. (b) As for (a), but the MMM of the CMIP5 models. (c) Difference in PW between the MMM of the CMIP5 models and observed PW (MMM minus the NVAP-C observation). (d) As for Fig. 2c, but difference in PW between the MMM of the CMIP5 models and another observed PW (MMM minus the RSS observation). PW was averaged over the 17-year period from 1989 to 2005. Both the historical simulations and observations are available.

robust model bias in PW over the higher SST regions where large amount of rainfalls are also observed. In addition, wet biases are simulated over the mid- and high-latitudes, which apparently reduce the global mean values of the dry bias. Therefore, the dry bias in the tropics is profound (Fig. 1b). Moreover, the biases near high mountain regions can be associated with the discrepancy between the smoothed orography in the climate models and the actual orography.

### *3.3 Dry biases caused by the SST bias*

As shown in Fig. 2c, there were negative PW biases over the warm SST regions and positive biases over the cold SST regions. In general, it is expected that PW is closely associated with SST since PW samples mainly low-level moisture that is strongly constrained to SST by the CC equation. To examine the simulated SST biases in the CGCMs, we also show the bias in PW simulated in the AMIP runs (Figs. 3, 4). The major differences in SST between CGCMs and AGCMs are arised from the air-sea interaction in CGCMs via Bjerknes feedback (e.g., Li and Xie 2014).

In the AMIP runs, the global mean dry bias of the MMM PW was reduced (Fig. 3a). Regarding the global mean values, the simulations by some of the models were wetter than the observation. To understand the reduction in the global mean dry bias, we examined the spatial distribution of the difference in PW (Fig. 4). In the AMIP runs, the dry bias of the MMM PW was partially reduced (Fig. 4) compared with the difference in PW in the coupled models (Fig. 2c), which indicates that the dry bias of PW was

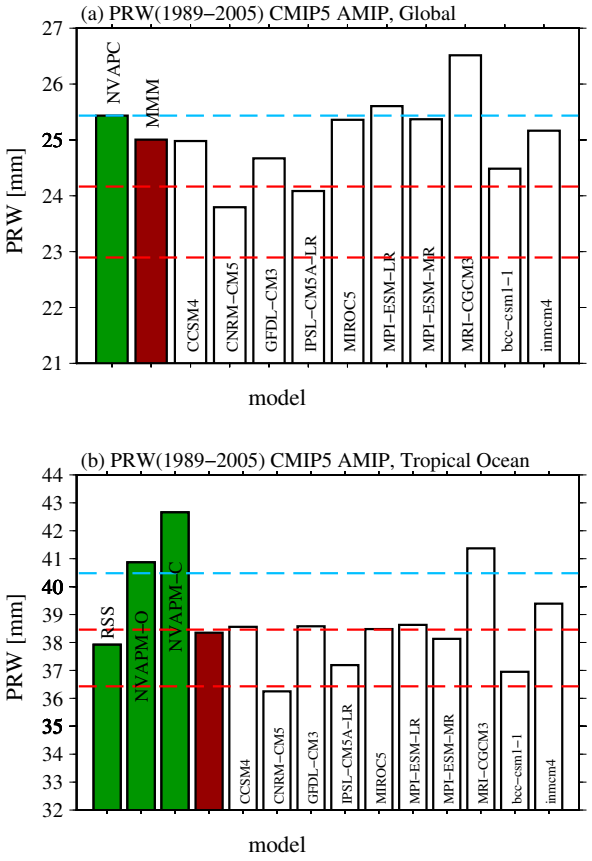


Fig. 3. As for Fig. 1, but for the Atmospheric Model Intercomparison Project (AMIP) simulations. MMM indicates a 10 model-ensemble mean of the AMIP climate models. Unit is mm.

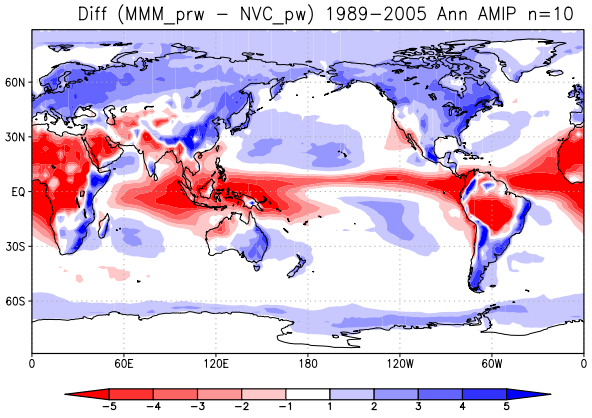


Fig. 4. As for Fig. 2c, but for the MMM of the AMIP runs (10 models) and observed (NVAP-C) PWs (MMM minus the NVAP-C observations). Unit is mm.

partially associated with the biases of SST. Nevertheless, the spatial distribution of the common dry bias of AMIP remained over the high PW regions in the tropics, which implies that there is still a distinct dry bias in the tropical regions, although the observed SSTs are prescribed (Fig. 3b). In addition, the AMIP models simulated stronger wet biases over the mid- and high-latitude regions, which contributed to cancellation of the global mean dry bias.

The spatial pattern of dry bias in the CMIP5 is very similar to that in AMIP runs, which implies that there is a common error of a physical process in both CMIP5 and AMIP runs. Therefore, it is possible that other factors contribute to the systematic dry biases in the CMIP5 climate models as well as AMIP runs.

### *3.4 Relationship between PW and rainfall characteristics*

We also investigated the biases of MMM PW as a function of the observed PW over the tropics, to quantify the characteristics of the simulated PW bias (Fig. 5a). The negative PW biases increased with the absolute values of the observed PW. When PW was larger than approximately 35 mm, dry biases were observed in most tropical grids. This result agreed with the spatial pattern of the PW bias (Fig. 2c). Note that the PW bias was significant over the wet region where PW values exceeded 35 mm. Apart from the major cluster in the scatterplot, a strong dry bias of 10 to 5 mm was sometimes observed when the PW value was approximately 20 mm, as seen over and around the Sahara. However, this strong dry bias over the Sahara was not certain because the observed PW values were very uncertain in that region due to a lack of observations.

We also examined the bias of the simulated precipitation over the tropics, as a function of PW (Fig. 5b). The positive precipitation biases increased with the absolute value of PW. Compared with the PW biases, the precipitation biases were less systematic, because the spatiotemporal distribution of precipitation is more complicated than that of PW. Nevertheless, positive precipitation biases were apparent when PW exceeded 35 mm. Moreover, the positive biases seemed to be reduced when PW exceeded 50 mm. The physical processes underlying the relationship between PW and precipitation biases are discussed in Section 4.

## 4. Discussion

Water vapor is the source of rainfall. The amount of water vapor and related moisture transport may affect the rainfall characteristics, which may be due to

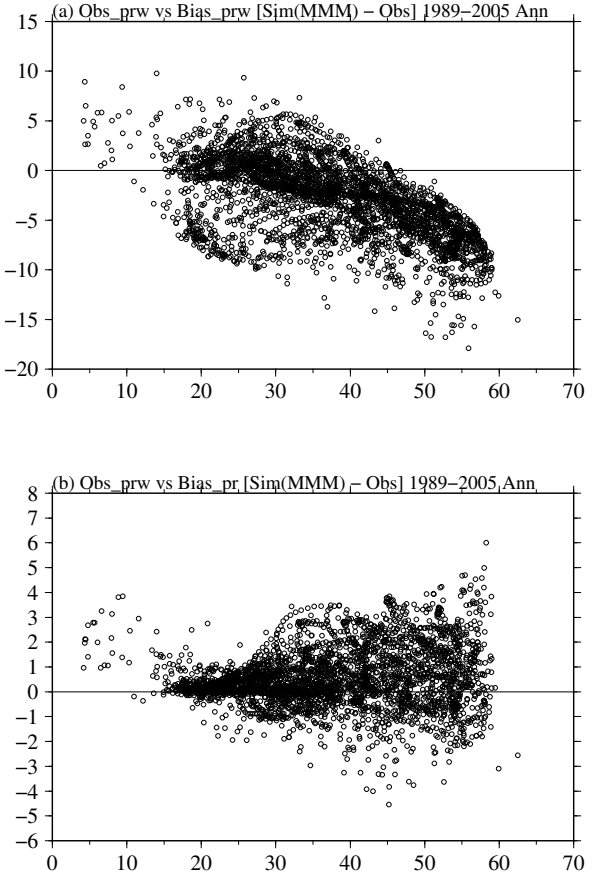


Fig. 5. (a) Scatterplot between the observed PW and the bias in PW over the tropics (30°S–30°N). (b) As for (a), but between the observed PW and the bias in precipitation. In both panels, 17-year climatological and annual mean values are plotted.

modulation of the development of tropical disturbances at various spatiotemporal scales, particularly over the tropics. On the other hand, rainfall characteristics affect the water vapor in the atmosphere. It may be significant how much water vapor is converted to rainfall. The two-dimensional histograms presented in Fig. 6 illustrate the relationship between water vapor (PW) and rainfall characteristics. For standardization, the occurrence frequency in each box is divided by the total occurrence frequency. To calculate the occurrence frequency, we used monthly mean values over a 204-month (17-year) period.

Higher frequencies are observed along the boxes with PW and rainfall of 45 mm and 1 mm day$^{-1}$, 50 mm and 3.5 mm day$^{-1}$, and 55 mm and 5 mm day$^{-1}$. Rainfall increases substantially when PW is greater than approximately 50 mm.

In most of the CMIP5 climate models used in this study, rainfall increases when PW is in the range 30 to 40 mm (Fig. 6). Rainfall increases dramatically when PW exceeds 40 mm. Although the pattern of the two-dimensional histograms is similar, the peak occurrence frequencies in the simulations are shifted in the direction of the lower PW values, and the curves are steeper when PW is in the range of 40 to 50 mm. Note that this tendency is common in the CMIP5 climate models.

Here, we propose two possible mechanisms. The first is that rainfall occurs in the CMIP5 climate models under lower PW conditions. Trenberth et al. (2011) showed that premature precipitation was dominant in CCSM4, which suggests that rainfall occurs under lower water vapor conditions. Rainfall onset in the CMIP5 climate models may be too sensitive to moist static energy (MSE). For CMIP5 climate models, the atmosphere is unable to hold as much water as the real atmosphere before precipitation occurs. Note that the bias of rainfall onset can be also associated with reproducibility of clouds, which may lead additional model biases.

Second, the CMIP5 climate models consume excessive water vapor or MSE for rainfall, which can be understood as the impact of rainfall characteristics on water vapor. This effect may decrease the amount of mean water vapor on a monthly time-scale. This explanation is also consistent with Trenberth et al. (2011). In addition, both of the mechanisms proposed here can occur simultaneously within a single climate model.

To understand the relationship between PW and rainfall characteristics, similar examination on the various time-scales and related regional moisture transport are necessary (e.g., Holloway and Neelin 2010; Liu et al. 2014; Allan et al. 2014) as a future study. Note that the understanding of the relationship may be related to changes in rainfall characteristics due to global warming (e.g., Trenberth et al. 2003).

## 5. Conclusions

This study assessed PW in the CMIP5 climate models using the NVAP-M global water vapor dataset. We also examined the relationship between water vapor and rainfall characteristics.

The results show that a systematic dry bias of PW is common in the CMIP5 climate models. The deficiency in PW is significant over wet regions where PW exceeds approximately 35 mm, mainly in the warm pool

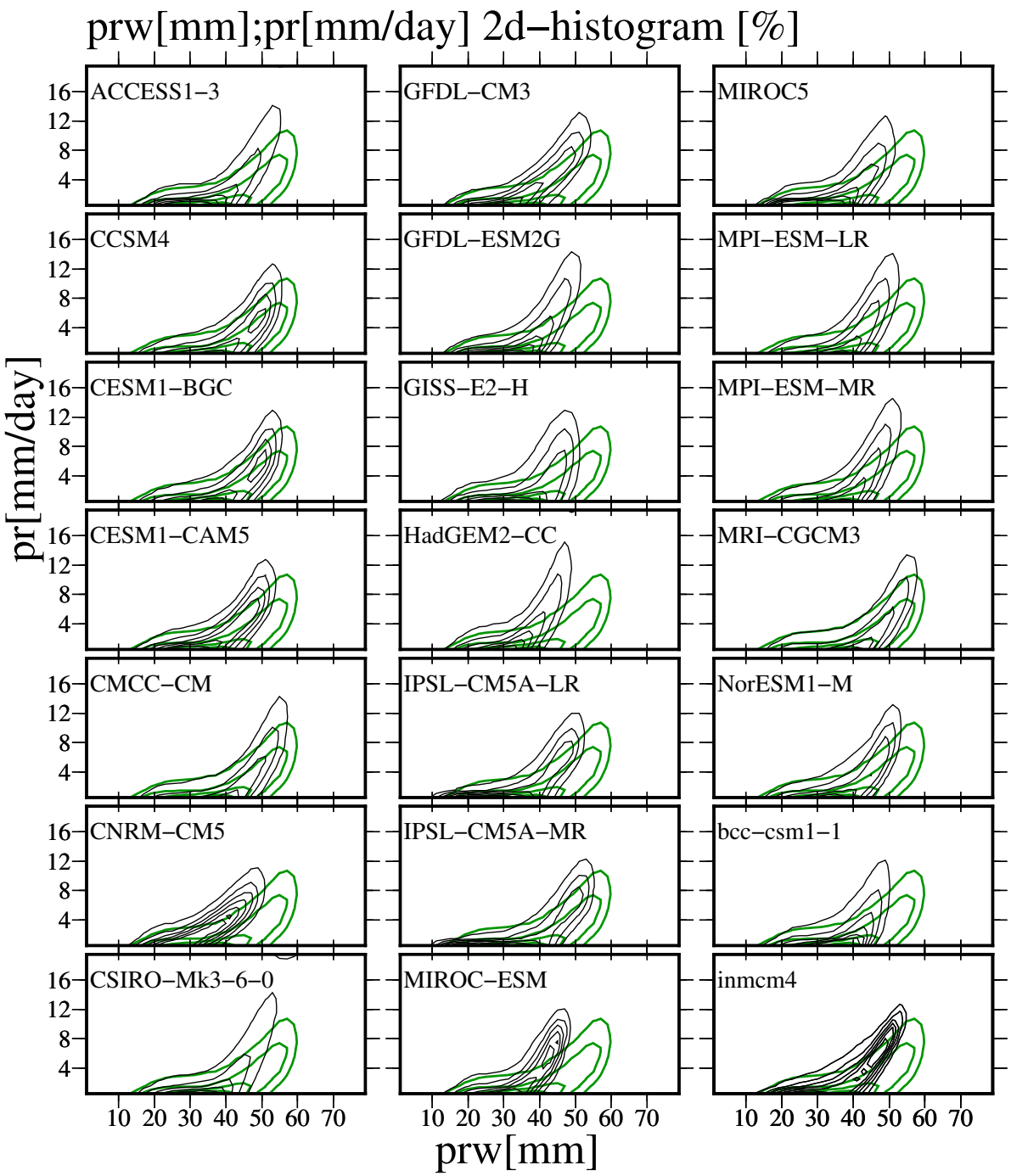


Fig. 6. Two-dimensional histogram between PW and precipitation over the tropics (30°S–30°N). The class width of PW is 2 mm from 0 to 80 mm. The class width of precipitation is 1 mm day$^{-1}$ from 0 to 20 mm day$^{-1}$. The green contours in each panel show the histogram between the observed PW and observed precipitation. The black contours in each panel show the histogram between the simulated PW and simulated precipitation. The name of the specific CMIP5 model is shown in each panel. In all panels, the occurrence frequency was calculated from monthly mean values over 204 months (17 years) on 2.5° × 2.5° grids over the tropics. The contour intervals are 0.2 %, from 0.2 % to 1.4 %. The smallest value of the contours is 0.2 %. The values are shown as percentages.

region. The dry biases are strong over climatologically warm SST regions, whereas wet biases are seen over climatologically cool SST regions. In addition, the dry biases are profound for all fields of water vapor, particularly over the tropical ocean. These systematic dry biases were reduced slightly in the AMIP runs, which indicates that the SST biases in the CMIP5 coupled climate models partially induce the dry biases. Nevertheless, profound dry biases remain over the tropics.

In most of the CMIP5 climate models used in this study, rainfall tends to occur under lower PW conditions compared with the observations. This situation may cause problems in the reproducibility of rainfall characteristics, e.g., rainfall consumes too much of the water vapor in the atmosphere. These possible mechanisms may explain the systematic dry bias. The results imply that the deficiency in simulated PW over the tropics is associated with the reproducibility of the rainfall characteristics in the CMIP5 models. Moreover, the spatial pattern of dry bias in the CMIP5 is very similar to that in AMIP runs, which can suggest the unrealistic rainfall characteristics, particularly over tropical regions. To understand the dry bias, the examinations of the reproducibility of rainfall characteristics on an event by event basis are required.

## Acknowledgments

The CMIP5 and GPCP datasets were provided by PCMDI and NOAA/OAR/ESRL/PSD, respectively. The author thanks three anonymous reviewers for constrictive comments. The author thanks Ms. Tomoko Motokado, Ms. Nozomi Kamizawa, and Dr. Daisaku Sakai for downloading and preprocessing the CMIP5 datasets. This work was partially supported by the MOE (2RF-1304), MEXT (GRENE-ei), and JAXA (PMM8-309), Japan.

## References

Adler, R. F., G. J. Huffman, A. Chang, R. Ferraro, P.-P. Xie, J. Janowiak, B. Rudolf, U. Schneider, S. Curtis, D. Bolvin, A. Gruber, J. Susskind, P. Arkin, and E. Nelkin, 2003: The version-2 Global Precipitation Climatology Project (GPCP) Monthly Precipitation Analysis (1979-present). *J. Hydrometeor.*, **4**, 1147–1167.

Allan, R. P., 2009: Examination of relationships between clear-sky longwave radiation and aspects of the atmospheric hydrological cycle in climate models, reanalyses, and observations. *J. Climate*, **22**, 3127–3145.

Allan, R. P., C. Liu, M. Zahn, D. A. Lavers, E. Koukouvagias, and A. Bodas-Salcedo, 2014: Physically consistent responses of the global atmospheric hydrological cycle in models and observations. *Surv. Geophys.*, **35**, 533–552.

Holloway, C. E., and J. D. Neelin, 2010: Temporal relations of column water vapor and tropical precipitation. *J. Atmos. Sci.*, **67**, 1091–1105.

Jiang, J. H., H. Su, C. Zhai, V. S. Perun, A. Del Genio, L. S. Nazarenko, L. J. Donner, L. Horowitz, C. Seman, J. Cole, A. Gettelman, M. A. Ringer, L. Rotstayn, S. Jeffrey, T. Wu, F. Brient, J.-L. Dufresne, H. Kawai, T. Koshiro, M. Watanabe, T. S. LÉcuyer, E. M. Volodin, T. Iversen, H. Drange, M. D. S. Mesquita, W. G. Read, J. W. Waters, B. Tian, J. Teixeira, and G. L. Stephens, 2012: Evaluation of cloud and water vapor simulations in CMIP5 climate models using NASA "A-Train" satellite observations. *J. Geophys. Res.*, **117**, D14105, doi:10.1029/2011JD017237.

John, V. O., and B. J. Soden, 2007: Temperature and humidity biases in global climate models and their impact on climate feedbacks. *Geophys. Res. Lett.*, **34**, L18704, doi:10.1029/2007GL030429.

Li, G., and S.-P. Xie, 2014: Tropical biases in CMIP5 multimodel ensemble: The excessive equatorial Pacific cold tongue and double ITCZ problems. *J. Climate*, **27**, 1765–1780.

Liu, C., R. P. Allan, M. Brooks, and S. Milton, 2014: Comparing tropical precipitation simulated by the Met Office NWP and climate models with satellite observations. *J. Appl. Meteor. Climatol.*, **53**, 200–214.

Mears, C. A., B. D. Santer, F. J. Wentz, K. E. Taylor, and M. F. Wehner, 2007: Relationship between temperature and precipitable water changes over tropical oceans. *Geophys. Res. Lett.*, **34**, L24709, doi:10.1029/2007GL031936.

Randel, D. L., T. H. Vonder Haar, M. A. Ringerud, G. L. Stephens, T. J. Greenwald, and C. L. Combs, 1996: A new global water vapor dataset. *Bull. Amer. Meteor. Soc.*, **77**, 1233–1246.

Schröder, M., M. Lockhoff, J. M. Forsythe, H. Q. Cronk, T. H. Vonder Haar, and R. Bennartz, 2016: The GEWEX water vapor assessment: Results from intercomparison, trend, and homogeneity analysis of total column water vapor. *J. Appl. Meteor. Climatol.*, **55**, 1633–1649.

Su, H., J. H. Jiang, C. Zhai, V. S. Perun, J. T. Shen, A. Del Genio, L. S. Nazarenko, L. J. Donner, L. Horowitz, C. Seman, C. Morcrette, J. Petch, M. Ringer, J. Cole, K. von Salzen, M. d. S. Mesquita, T. Iversen, J. E. Kristjansson, A. Gettelman, L. Rotstayn, S. Jeffrey, J.-L. Dufresne, M. Watanabe, H. Kawai, T. Koshiro, T. Wu, E. M. Volodin, T. L'Ecuyer, J. Teixeira, and G. L. Stephens, 2013: Diagnosis of regime-dependent cloud simulation errors in CMIP5 models using "A-Train" satellite observations and reanalysis data. *J. Geophys. Res.*, **118**, 2762–2780.

Takahashi, H. G., M. Hara, M. Fujita, and T. Yoshikane, 2012: A discrepancy in precipitable water among reanalyses and the impact of forcing dataset on downscaling in the tropics. *Atmos. Chem. Phys. Discuss.*, **12**, 23759–23791.

Taylor, K. E., R. J. Stouffer, and G. A. Meehl, 2012: An overview of CMIP5 and the experiment design. *Bull. Amer. Meteor. Soc.*, **93**, 485–498.

Tian, B., E. J. Fetzer, B. H. Kahn, J. Teixeira, E. Manning, and T. Hearty, 2013: Evaluating CMIP5 models using

AIRS tropospheric air temperature and specific humidity climatology. *J. Geophys. Res.*, **118**, 114–134.

Trenberth, K. E., A. Dai, R. M. Rasmussen, and D. B. Parsons, 2003: The changing character of precipitation. *Bull. Amer. Meteor. Soc.*, **84**, 1205–1217.

Trenberth, K. E., J. Fasullo, and L. Smith, 2005: Trends and variability in column-integrated atmospheric water vapor. *Climate Dyn.*, **24**, 741–758.

Trenberth, K. E., J. T. Fasullo, and J. Mackaro, 2011: Atmospheric moisture transports from ocean to land and global energy flows in reanalyses. *J. Climate*, **24**, 4907–4924.

Vonder Haar, T. H., J. L. Bytheway, and J. M. Forsythe, 2012: Weather and climate analyses using improved global water vapor observations. *Geophys. Res. Lett.*, **39**, L15802, doi:10.1029/2012GL052094.

Wentz, F. J., 1997: A well-calibrated ocean algorithm for special sensor microwave/imager. *J. Geophys. Res.*, **102**, 8703–8718.

Wentz, F. J., and M. Schabel, 2000: Precise climate monitoring using complementary satellite data sets. *Nature*, **403**, 414–416.

Wentz, F. J., L. Ricciardulli, K. Hilburn, and C. Mears, 2007: How much more rain will global warming bring? *Science*, **317**, 233–235.